TIME-DEPENDENT THREE DIMENSIONAL STRETCHED FLOW OF A JEFFREY FLUID WITH HEAT SOURCE/SINK

Manzoor Ahmad[a], Iftikhar Ahmad[a] and Muhammad Sajid[b]
[a]Department of Mathematics, University of Azad Jammu & Kashmir, Muzaffarabad 13100, Pakistan
[b]Theoretical Physics Division, PINSTECH, P.O. Nilore, Islamabad 44000, Pakistan
[+]Corresponding author: manzoorajku@gmail.com

ABSTRACT*: *This article addresses the unsteady three dimensional flow of a Jeffrey fluid with heat transfer effects. Flow is caused due to unsteady stretched surface. Heat transfer through constant temperature (CT) and constant heat flux (CH) is considered. In addition the heat transfer rate varies along the surface. Homotopy analysis method (HAM) is implemented for obtaining the convergent series solutions of the transformed equations. The behavior of fluid velocity, temperature and Nusselt number are analyzed against the pertinent parameters of interest. The finding indicates that there is reduction in temperature and thermal boundary layer. The boundary layer thickness is reduced if the sheet temperature increases in one or both of the lateral directions. The comparison of the obtained solution with existing results in special case is found in excellent agreement.

Keywords: Jeffery fluid, Unsteady flow, heat transfer analysis, bidirectional stretching, HAM.

1. INTRODUCTION

The study of fluids having nonlinear relationship between the shear stress and rate of deformation is a topic of great interest for many researchers working in the field for the past two decade. The reason of increasing interest lays in the fact that the linear relationship between shear stress and rate of deformation is not valid for most the fluids that exist in nature, industry and technology. Furthermore, the phenomena like normal stress effects, shear thinning and thickening, time relaxation and retardation, rotation of microelement, effect of couple stresses cannot be explained through the Navier-Stokes equations. Therefore, a need for more complex constitutive relationship is the need of time. However, the complex natures of fluids that exist make it impossible to describe these nonlinear effects by a single constitutive relationship. Hence, different models of such fluids are introduced by the various investigators [1-6]. The initial problem of two dimensional flows due to a stretching plane surface is discussed by Crane [7]. To date many researches have been done on steady boundary layer problems due to a stretching sheet. Namely, Wang [8] and Ariel [9] studied steady three dimensional boundary layer flows over a stretching surface. Liu and Andersson [10] investigated the heat transfer over a stretching surface with variable thermal conditions. Ahmad *et al*. [11] added magnetic effect to the flow over a steady stretching sheet in a porous medium. Further Hayat *et al*. [12] considered three dimensional flow over a stretching surface in a viscoelastic fluid. In another article Hayat et al. [13] discussed three dimensional stretched flow of Jeffery fluid with variable thermal conductivity and thermal radiation. Shehzad *et al*. [14] explained MHD three dimensional flow of Jeffery fluid with Newtonian heating. On the other hand, only a few studies have been reported on the problem of unsteady boundary layer flow due to a stretching sheet. Surma Devi *et al* [15] and Lakshimsha *et al* [16] studied unsteady three dimensional boundary layer flows over a stretching surface. Ali *et al* [17] investigated the unsteady uniform flow across a stretching surface in an arbitrary direction, where the unsteadiness is caused by the impulsive motion of the stretching surface. While, Abd El-Aziz [18] added radiation effect to the flow over an unsteady stretching sheet and reported that for larger Prandtl number, the effect of radiation parameter becomes more significant. Hayat *et al* [19] studied the time dependent three dimensional flow of elastico viscous fluid and mass transfer over a bidirectional stretching sheet. Recently Awais *et al*. [20] studied time dependent boundary layer flow of a Maxwell fluid over an unsteady bidirectional stretching sheet. Very recently Ahmad *et al.* [21] discussed heat transfer analysis of MHD flow due to unsteady bidirectional stretching sheet through porous space. The present paper aims to study the problem of time dependent three dimensional Jeffrey fluid and heat transfer across an unsteady bidirectional stretching sheet with variable thermal conditions. Jeffrey fluid is a subclass of non-Newtonian fluids which capable of describing ratio of relaxation times to retardation time. To the best of our knowledge the present problem has not been considered before and thus the reported results are new. The transformed equations are solved analytically via homotopic solutions [22-30]. The obtained results are analyzed.

2. PROBLEM FORMULATIONS

We consider time dependent three dimensional flow of an incompressible Jeffrey fluid over an unsteady stretching surface. The flow occupies the region $z > 0$ and coincide the space perpendicular to xy −plane. The motion in the fluid is caused by a non-conducting stretching sheet. The constitutive equations for the Jeffery fluid model are

$$\boldsymbol{T} = -p\boldsymbol{I} + \boldsymbol{S}, \tag{1}$$

$$\boldsymbol{S} = \frac{\mu}{1+\lambda_1}(\dot{\boldsymbol{r}} + \lambda_2\ddot{\boldsymbol{r}}), \tag{2}$$

where $\boldsymbol{T}$ denote the stress tensor, p denote the pressure, $\boldsymbol{I}$ the identity tensor, $\boldsymbol{S}$ the extra stress tensor, μ the dynamic viscosity, λ_1 the ratio of relaxation and retardation times and λ_2 the retardation time. More over the dots over the quantities denote the material differentiation. The quantities $\dot{\boldsymbol{r}}$ and $\ddot{\boldsymbol{r}}$ are defined as

$$\dot{\boldsymbol{r}} = \nabla\boldsymbol{V} + (\nabla\boldsymbol{V})^{\boldsymbol{T}}, \tag{3}$$

$$\ddot{\boldsymbol{r}} = \frac{d}{dt}\dot{\boldsymbol{r}}, \tag{4}$$

The law of conservation of mass and momentum for present flow problem are given by [31]

$$\frac{\partial u}{\partial x} + \frac{\partial v}{\partial y} + \frac{\partial w}{\partial z} = 0, \tag{5}$$

$$\begin{aligned}
&\frac{\partial u}{\partial t}+u\frac{\partial u}{\partial x}+v\frac{\partial u}{\partial y}+w\frac{\partial u}{\partial z}=\frac{\nu}{1+\lambda_1}\bigg[\frac{\partial^2 u}{\partial x^2}+\frac{\partial^2 u}{\partial y^2}+\frac{\partial^2 u}{\partial z^2}+\\
&\lambda_2\bigg(2\frac{\partial^3 u}{\partial x^2\partial t}+\frac{\partial^3 u}{\partial y^2\partial t}+\frac{\partial^3 u}{\partial z^2\partial t}+\frac{\partial^3 v}{\partial x\partial y\partial t}+\frac{\partial^3 w}{\partial x\partial z\partial t}+2\frac{\partial u}{\partial x}\frac{\partial^2 u}{\partial x^2}+\\
&2u\frac{\partial^3 u}{\partial z^3}+2\frac{\partial v}{\partial x}\frac{\partial^2 u}{\partial x\partial y}+2v\frac{\partial^3 u}{\partial x^2\partial y}+2\frac{\partial w}{\partial x}\frac{\partial^2 u}{\partial x\partial z}+2w\frac{\partial^3 u}{\partial x^2\partial z}+\\
&\frac{\partial u}{\partial y}\frac{\partial^2 u}{\partial x\partial y}+u\frac{\partial^3 u}{\partial y^2\partial x}+\frac{\partial u}{\partial y}\frac{\partial^2 v}{\partial x^2}+u\frac{\partial^3 v}{\partial x^2\partial y}+\frac{\partial v}{\partial y}\frac{\partial^2 u}{\partial y^2}+v\frac{\partial^3 u}{\partial y^3}+\\
&\frac{\partial v}{\partial y}\frac{\partial^2 v}{\partial x\partial y}+v\frac{\partial^3 v}{\partial y^2\partial x}+\frac{\partial w}{\partial y}\frac{\partial^2 u}{\partial y\partial z}+w\frac{\partial^3 u}{\partial y^2\partial z}+\frac{\partial w}{\partial y}\frac{\partial^2 v}{\partial x\partial z}+\\
&w\frac{\partial^3 v}{\partial x\partial y\partial z}+u\frac{\partial^3 u}{\partial z^2\partial y}+\frac{\partial u}{\partial z}\frac{\partial^2 u}{\partial x\partial z}+u\frac{\partial^3 w}{\partial x^2\partial z}+\frac{\partial u}{\partial z}\frac{\partial^2 w}{\partial x^2}+v\frac{\partial^3 u}{\partial z^2\partial y}+\\
&\frac{\partial v}{\partial z}\frac{\partial^2 u}{\partial y\partial z}+v\frac{\partial^3 w}{\partial x\partial y\partial z}+\frac{\partial v}{\partial z}\frac{\partial^2 w}{\partial y\partial x}+w\frac{\partial^3 u}{\partial z^3}+\frac{\partial w}{\partial z}\frac{\partial^2 u}{\partial z^2}+w\frac{\partial^3 w}{\partial z^2\partial x}+\\
&\frac{\partial w}{\partial z}\frac{\partial^2 w}{\partial x\partial z}\bigg)\bigg], \qquad (6)
\end{aligned}$$

$$\begin{aligned}
&\frac{\partial v}{\partial t}+u\frac{\partial v}{\partial x}+v\frac{\partial v}{\partial y}+w\frac{\partial v}{\partial z}=\frac{\nu}{1+\lambda_1}\bigg[\frac{\partial^2 v}{\partial x^2}+\frac{\partial^2 v}{\partial y^2}+\frac{\partial^2 v}{\partial z^2}+\\
&\lambda_2\bigg(2\frac{\partial^3 v}{\partial y^2\partial t}+\frac{\partial^3 v}{\partial x^2\partial t}+\frac{\partial^3 v}{\partial z^2\partial t}+\frac{\partial^3 u}{\partial x\partial y\partial t}+\frac{\partial^3 w}{\partial y\partial z\partial t}+2\frac{\partial v}{\partial y}\frac{\partial^2 v}{\partial y^2}+\\
&2v\frac{\partial^3 v}{\partial y^3}+2\frac{\partial u}{\partial y}\frac{\partial^2 v}{\partial x\partial y}+2u\frac{\partial^3 v}{\partial y^2\partial x}+2\frac{\partial w}{\partial y}\frac{\partial^2 v}{\partial y\partial z}+2w\frac{\partial^3 v}{\partial y^2\partial z}+\\
&\frac{\partial u}{\partial x}\frac{\partial^2 u}{\partial x\partial y}+u\frac{\partial^3 u}{\partial x^2\partial y}+\frac{\partial u}{\partial x}\frac{\partial^2 v}{\partial x^2}+v\frac{\partial^3 v}{\partial y^2\partial x}+\frac{\partial v}{\partial x}\frac{\partial^2 u}{\partial y^2}+u\frac{\partial^3 v}{\partial x^3}+\\
&\frac{\partial u}{\partial x}\frac{\partial^2 u}{\partial x\partial y}+v\frac{\partial^3 v}{\partial x^2\partial y}+\frac{\partial v}{\partial x}\frac{\partial^2 v}{\partial y\partial z}+w\frac{\partial^3 v}{\partial x^2\partial z}+\frac{\partial w}{\partial x}\frac{\partial^2 u}{\partial y\partial z}+w\frac{\partial^3 u}{\partial x\partial y\partial z}+\\
&u\frac{\partial^3 v}{\partial z^2\partial x}+\frac{\partial u}{\partial z}\frac{\partial^2 v}{\partial x\partial z}+u\frac{\partial^3 w}{\partial x\partial y\partial z}+\frac{\partial u}{\partial z}\frac{\partial^2 w}{\partial x\partial y}+v\frac{\partial^3 v}{\partial z^2\partial y}+\frac{\partial v}{\partial z}\frac{\partial^2 v}{\partial y\partial z}+\\
&v\frac{\partial^3 w}{\partial y^2\partial z}+\frac{\partial v}{\partial z}\frac{\partial^2 w}{\partial y^2}+w\frac{\partial^3 v}{\partial z^3}+\frac{\partial w}{\partial z}\frac{\partial^2 v}{\partial z^2}+w\frac{\partial^3 w}{\partial z^2\partial y}+\frac{\partial w}{\partial z}\frac{\partial^2 w}{\partial y\partial z}\bigg)\bigg], \qquad (7)
\end{aligned}$$

$$\begin{aligned}
&\frac{\partial w}{\partial t}+u\frac{\partial w}{\partial x}+v\frac{\partial w}{\partial y}+w\frac{\partial w}{\partial z}=\frac{\nu}{1+\lambda_1}\bigg[\frac{\partial^2 w}{\partial x^2}+\frac{\partial^2 w}{\partial y^2}+\frac{\partial^2 w}{\partial z^2}+\\
&\lambda_2\bigg(\frac{\partial^3 w}{\partial x^2\partial t}+\frac{\partial^3 w}{\partial y^2\partial t}+2\frac{\partial^3 w}{\partial z^2\partial t}+\frac{\partial^3 u}{\partial x\partial z\partial t}+\frac{\partial^3 v}{\partial y\partial z\partial t}+u\frac{\partial^3 u}{\partial x^2\partial z}+\\
&\frac{\partial u}{\partial x}\frac{\partial^2 u}{\partial x\partial z}+u\frac{\partial^3 w}{\partial x^3}+\frac{\partial u}{\partial x}\frac{\partial^2 w}{\partial x^2}+v\frac{\partial^3 u}{\partial x\partial y\partial z}+\frac{\partial v}{\partial x}\frac{\partial^2 u}{\partial y\partial z}+v\frac{\partial^3 w}{\partial x^2\partial y}+\\
&\frac{\partial v}{\partial x}\frac{\partial^2 w}{\partial y\partial z}+w\frac{\partial^3 u}{\partial z^2\partial x}+\frac{\partial w}{\partial x}\frac{\partial^2 u}{\partial z^2}+w\frac{\partial^3 w}{\partial x^2\partial z}+\frac{\partial w}{\partial x}\frac{\partial^2 w}{\partial z\partial x}+u\frac{\partial^3 v}{\partial x\partial y\partial z}+\\
&\frac{\partial u}{\partial y}\frac{\partial^2 v}{\partial x\partial z}+u\frac{\partial^3 w}{\partial x\partial y^2}+\frac{\partial u}{\partial y}\frac{\partial^2 w}{\partial x\partial y}+v\frac{\partial^3 v}{\partial y^2\partial z}+\frac{\partial v}{\partial y}\frac{\partial^2 v}{\partial y\partial z}+v\frac{\partial^3 w}{\partial y^3}+\\
&\frac{\partial v}{\partial y}\frac{\partial^2 w}{\partial y^2}+w\frac{\partial^3 v}{\partial z^2\partial y}+\frac{\partial w}{\partial y}\frac{\partial^2 v}{\partial z^2}+w\frac{\partial^3 w}{\partial y^2\partial z}+\frac{\partial w}{\partial y}\frac{\partial^2 w}{\partial y\partial z}+2u\frac{\partial^3 w}{\partial z^2\partial x}+\\
&2\frac{\partial u}{\partial z}\frac{\partial^2 w}{\partial x\partial z}+2v\frac{\partial^3 w}{\partial y^2\partial y}+2\frac{\partial v}{\partial y}\frac{\partial^2 w}{\partial y\partial z}+2w\frac{\partial^3 w}{\partial z^3}+\frac{\partial w}{\partial z}\frac{\partial^2 w}{\partial z^2}\bigg)\bigg], \qquad (8)
\end{aligned}$$

Invoking the boundary layer approximation [19-21]

$$u=O(1),\, v=O(1),\, x=O(1),\, y=O(1),\, w=O(\delta),\, z=O(\delta), \qquad (9)$$

Eqs. (6) and (7) takes the following equation and Eq. (8) vanishes as its every term has order δ.

$$\frac{\partial u}{\partial t}+u\frac{\partial u}{\partial x}+v\frac{\partial u}{\partial y}+w\frac{\partial u}{\partial z}=\frac{\nu}{1+\lambda_1}\left[\frac{\partial^2 u}{\partial z^2}+\lambda_2\begin{pmatrix}\frac{\partial^3 u}{\partial z^2\partial t}+u\frac{\partial^3 u}{\partial x\partial z^2}+v\frac{\partial^3 u}{\partial y\partial z^2}+\\ w\frac{\partial^3 u}{\partial z^3}+\frac{\partial u}{\partial z}\frac{\partial^2 u}{\partial x\partial z}+\frac{\partial v}{\partial z}\frac{\partial^2 u}{\partial y\partial z}+\frac{\partial w}{\partial z}\frac{\partial^2 u}{\partial z^2}\end{pmatrix}\right], \qquad (10)$$

$$\frac{\partial v}{\partial t}+u\frac{\partial v}{\partial x}+v\frac{\partial v}{\partial y}+w\frac{\partial v}{\partial z}=\frac{\nu}{1+\lambda_1}\left[\frac{\partial^2 v}{\partial z^2}+\lambda_2\begin{pmatrix}\frac{\partial^3 v}{\partial z^2\partial t}+u\frac{\partial^3 v}{\partial x\partial z^2}+v\frac{\partial^3 v}{\partial y\partial z^2}+\\ w\frac{\partial^3 v}{\partial z^3}+\frac{\partial u}{\partial z}\frac{\partial^2 v}{\partial x\partial z}+\frac{\partial v}{\partial z}\frac{\partial^2 v}{\partial y\partial z}+\frac{\partial w}{\partial z}\frac{\partial^2 v}{\partial z^2}\end{pmatrix}\right], \qquad (11)$$

$$\frac{\partial T}{\partial t}+u\frac{\partial T}{\partial x}+v\frac{\partial T}{\partial y}+w\frac{\partial T}{\partial z}=k_1\frac{\partial^2 T}{\partial z^2}+\frac{Q}{\rho c_p}(T-T_\infty). \qquad (12)$$

The boundary conditions relevant to the present flow situation are

$$u=u_w(x)=\frac{ax}{1-ct},\ \ v=v_w(y)=\frac{by}{1-ct},\ \ w=0,\ \text{ at } z=0,$$

$$u\to 0,\ \ v\to 0,\ \text{ as } z\to\infty. \qquad (13)$$

For the temperature we have the following two sets of boundary conditions.

(CT case): $T=T_{w(x,y)}=T_\infty+Ax^r y^s$ at $z=0$,

$T\to T_\infty$ as $y\to\infty$. (14)

(CH case): $-\lambda_3\frac{\partial T}{\partial z} = Bx^r y^s$ at $z=0$, $T\to T_\infty$ as $y\to\infty$. (15)

Here $a>0$, $b>0$ and $c>0$ are constant stretching rates with dimension time^{-1} such that $ct<1$, ν is the kinematic viscosity. Note that $u=u_w(x)$ and $v=v_w(y)$ are the unsteady stretching velocities along $x-$ and $y-$direction respectively whereas when $z\to\infty$ then both $u\to 0$ and $v\to 0$ means that fluid is rest for away from the sheet and major contribution of the flow occur only in the boundary layer. That is why we have employed the order analysis and analyze the results in boundary layer region. The stretching phenomenon in this direction has already studied by various authors [11,12,13,14,19,20,21]. We define the following similarity variables

$$\eta=\sqrt{\frac{a}{\nu(1-ct)}}z,\ \ u=\frac{ax}{1-ct}f'(\eta),\ \ v=\frac{by}{1-ct}g'(\eta),\ \ w=-\sqrt{\frac{a\nu}{1-ct}}\{f(\eta)+g(\eta)\}, \qquad (16)$$

$$\theta(\eta)=\frac{T(x,y,z,t)-T_\infty}{T_w(x,y)-T_\infty},\ \text{[CT]} \quad \text{and} \quad T(x,y,z,t)-T_\infty=\frac{B}{\lambda_3}\sqrt{\frac{\nu}{a}}x^r y^s\phi(\eta),\ \text{[CH]}. \qquad (17)$$

where λ_3 is the thermal conductivity of the fluid, T_∞ is the ambient temperature outside the thermal boundary layer, A and B are positive constants. The power indices r and s decided how the temperature or the heat flux at the sheet varies in the (x,y)-plane.

Thus the Eq. (5) is identically satisfied and Eqs. (10-12) take the following form

$$f''' + (1+\lambda_1)\left[(f+g)f'' - f'^2 - A\left(f' + \frac{\eta}{2}f''\right)\right] + \beta_1[f''^2 - (f+g)f''' - g'f''' + A(2f''' + \eta f'''')] = 0, \quad (18)$$

$$g''' + (1+\lambda_1)\left[(f+g)g'' - f'^2 - A\left(g' + \frac{\eta}{2}g''\right)\right] + \beta_1[g''^2 - (f+g)g'''' - f'g''' + A(2g''' + \eta g'''')] = 0, \quad (19)$$

$$\theta'' + Pr(f+g)\theta' + Pr(\beta - rf' - sg')\,\theta - \mathrm{A}\left(\frac{\eta}{2}\theta' - \theta\right)Pr = 0, \quad \text{[CT]}, \quad (20)$$

$$\phi'' + Pr(f+g)\phi' + Pr(\beta - rf' - sg')\,\phi - \mathrm{A}\left(\frac{\eta}{2}\phi' - \phi\right)Pr = 0, \quad \text{[CH]}. \quad (21)$$

The associated boundary conditions are also reduced into the following form

$$f = 0, g = 0, g' = \alpha, \theta = 1, \phi' = -1, \text{ at } \eta = 0,$$
$$f' \to 0,\ g' \to 0, \theta \to 0, \phi \to 0, \text{ as } \eta \to \infty, \quad (22)$$

$$\alpha = \frac{b}{a},\ A = \frac{c}{a},\ \beta_1 = \frac{\lambda_2 a}{1-ct}\ \ Pr = \frac{\nu}{k},\ \beta = \frac{Q}{\rho C_p a}. \quad (23)$$

The local Nusselt number in dimensionless form is

$$\frac{Nu}{Re_x^{1/2}} = -\theta'(0), \quad (24)$$

where $Re_x = \frac{u_w(x)}{\nu}$, is the local Reynolds number.

3. HOMOTOPY ANALYSIS SOLUTIONS AND CONVERGENCE ANALYSIS

Choose the initial approximations and linear operators given below

$$f_0(\eta) = 1 - \exp(\eta), g_0(\eta) = \alpha(1 - \exp(-\eta)), \theta_0(\eta) = \exp(-\eta), \phi_0(\eta) = \exp(-\eta), \quad (25)$$

$$\mathcal{L}_1(f) = \frac{d^3 f}{d\eta^3} - \frac{df}{d\eta},\ \mathcal{L}_2(g) = \frac{d^3 g}{d\eta^3} - \frac{dg}{d\eta},\ \mathcal{L}_3(\theta) = \frac{d^2\theta}{d\eta^2} - \theta$$
$$\text{and } \mathcal{L}_4(\phi) = \frac{d^2\phi}{d\eta^2} - \phi, \quad (26)$$

satisfynig

$$\begin{cases} \mathcal{L}_1[C_1 + C_2\exp(\eta) + C_3\exp(-\eta)] = 0, \\ \mathcal{L}_2[C_4 + C_5\exp(\eta) + C_6\exp(-\eta)] = 0, \\ \mathcal{L}_3[C_7\exp(\eta) + C_8\exp(-\eta)] = 0, \\ \mathcal{L}_4[C_9\exp(\eta) + C_{10}\exp(-\eta)] = 0, \end{cases} \quad (27)$$

in which $C_i's$ are arbitrary constants. From Eqs. (18)–(21), the nonlinear operators $\mathcal{N}_f, \mathcal{N}_g, \mathcal{N}_\theta$ *and* $\mathcal{N}_\phi$ are defined by the following expressions

$$\mathcal{N}_f[\hat f(\eta,p), \hat g(\eta,p)] = \hat f'''(\eta,p) + (1+\lambda_1)\left\{\left(\hat f(\eta,p) + \hat g(\eta,p)\right)\hat f''(\eta,p) - \left(\hat f'(\eta,p)\right)^2 - A\left\{\frac{\eta}{2}\hat f''(\eta,p) + \hat f'(\eta,p)\right\}\right\} - \beta_1\left\{\hat f''^2(\eta,p) - \left(\hat f(\eta,p) + \hat g(\eta,p)\right)\hat f'''(\eta,p) - \hat g'(\eta,p)\hat f'''(\eta,p) + A\left(\eta\hat f''''(\eta,p) + 2\hat f'''(\eta,p)\right)\right\}, \quad (28)$$

$$\mathcal{N}_g[\hat f(\eta,p), \hat g(\eta,p)] = \hat g'''(\eta,p) + (1+\lambda_1)\left\{\left(\hat f(\eta,p) + \hat g(\eta,p)\right)\hat g''(\eta,p) - \left(\hat g'(\eta,p)\right)^2 - A\left\{\frac{\eta}{2}\hat g''(\eta,p) + \hat g'(\eta,p)\right\}\right\} - \beta_1\left\{\hat g''^2(\eta,p) - \left(\hat f(\eta,p) + \hat g(\eta,p)\right)\hat g'''(\eta,p) - \hat f'(\eta,p)\hat g'''(\eta,p) + A\left(\eta\hat g''''(\eta,p) + 2\hat g'''(\eta,p)\right)\right\}, \quad (29)$$

$$\mathcal{N}_\theta[\hat f(\eta,p), \hat g(\eta,p)] = \hat\theta''(\eta,p) + Pr\left\{\begin{array}{c} \left(\hat f(\eta,p) + \hat g(\eta,p)\right)\hat\theta'(\eta,p) \\ + \begin{pmatrix} \beta - r\hat f'(\eta,p) \\ -s\hat g'(\eta,p) \end{pmatrix}\hat\theta(\eta,p) \\ -A\left(\frac{\eta}{2}\hat\theta'(\eta,p) + \hat\theta(\eta,p)\right) \end{array}\right\}, \quad (30)$$

$$\mathcal{N}_\phi[\hat f(\eta,p), \hat g(\eta,p)] = \hat\phi''(\eta,p) + Pr\left\{\begin{array}{c} \left(\hat f(\eta,p) + \hat g(\eta,p)\right)\hat\phi'(\eta,p) \\ + \begin{pmatrix} \beta - r\hat f'(\eta,p) \\ -s\hat g'(\eta,p) \end{pmatrix}\hat\phi(\eta,p) \\ -A\left(\frac{\eta}{2}\hat\phi'(\eta,p) + \hat\phi(\eta,p)\right) \end{array}\right\}. \quad (31)$$

If $p \in [0,1]$ is the embedding parameter and $\hbar_f, \hbar_g, \hbar_\theta$ *and* $\hbar_\phi$ are the non-zero auxiliary parameters, then the zeroth-order deformation problems are of the following form

$$(1-p)\mathcal{L}_1[\hat f(\eta,p) - f_0(\eta)] = p\hbar_f\mathcal{N}_f, \quad (32)$$
$$(1-p)\mathcal{L}_1[g(\eta,p) - g_\circ(\eta)] = p\hbar_g\mathcal{N}_g, \quad (33)$$
$$(1-p)\mathcal{L}_2[\hat\theta(\eta,p) - \theta_0(\eta)] = p\hbar_\theta\mathcal{N}_\theta, \quad (34)$$
$$(1-p)\mathcal{L}_2[\hat\phi(\eta,p) - \phi_0(\eta)] = p\hbar_\phi\mathcal{N}_\phi, \quad (35)$$
$$\hat f(0,p) = \hat g(0,p) = 0, \hat f'(0,p) = 1,$$
$$\hat g'(0,p) = \alpha, \hat\theta(0,p) = 1, \phi'(0,p) = -1, \quad (36)$$
$$\hat f'(\infty,p) = \hat g'(\infty,p) = \hat\theta(\infty,p) = \hat\phi(\infty,p) = 0. \quad (37)$$

These equations implies that for $p = 0$ and $p = 1$ have the following solutions

$$\hat f(\eta,0) = f_0(\eta),\ \hat f(\eta,1) = f(\eta), \quad (38)$$
$$\hat g(\eta,0) = g_0(\eta),\ \hat g(\eta,1) = g(\eta), \quad (39)$$
$$\hat\theta(\eta,0) = \theta_0(\eta),\ \hat\theta(\eta,1) = \theta(\eta), \quad (40)$$
$$\hat\phi(\eta,0) = \phi_0(\eta),\ \hat\phi(\eta,1) = \phi(\eta). \quad (41)$$

$\hat f(\eta,p)$, $\hat g(\eta,p)$, $\hat\theta(\eta,p)$ and $\hat\phi(\eta,p)$ varies from $f_0(\eta), g_0(\eta)$, $\theta_0(\eta)$ and $\phi_0(\eta)$ to the solutions $f(\eta)$, $g(\eta)$, $\theta(\eta)$ and $\phi(\eta)$ as p varies from 0 to 1. The Taylor's series thus suggest that

$$\hat f(\eta,p) = f_0(\eta) + \sum_{m=1}^{\infty} f_m(\eta)p^m,$$
$$f_m(\eta) = \frac{1}{m!}\frac{\partial^m \hat f(\eta,p)}{\partial p^m}\Big|_{p=0}, \quad (42)$$

$$\hat g(\eta,p) = g_0(\eta) + \sum_{m=1}^{\infty} g_m(\eta)p^m,$$
$$g_m(\eta) = \frac{1}{m!}\frac{\partial^m \hat g(\eta,p)}{\partial p^m}\Big|_{p=0}, \quad (43)$$

$$\hat\theta(\eta,p) = \theta_0(\eta) + \sum_{m=1}^{\infty} \theta_m(\eta)p^m,$$
$$\theta_m(\eta) = \frac{1}{m!}\frac{\partial^m \hat\theta(\eta,p)}{\partial p^m}\Big|_{p=0}, \quad (44)$$

$$\hat\phi(\eta,p) = \phi_0(\eta) + \sum_{m=1}^{\infty} \phi_m(\eta)p^m,$$
$$\phi_m(\eta) = \frac{1}{m!}\frac{\partial^m \hat\phi(\eta,p)}{\partial p^m}\Big|_{p=0}, \quad (45)$$

The auxiliary parameters $\hbar_f, \hbar_g, \hbar_\theta$ *and* $\hbar_\phi$ in Eqs. (32)-(35) ensures the the convergence of the series solutions given by Eqs. (42)-(45). Assuming that $\hbar_f, \hbar_g, \hbar_\theta$ *and* $\hbar_\phi$ are chosen such that the series in Eqs. (42)-(45) are convergent at $p = 1$. Thus

$$\hat{f}(\eta) = f_0(\eta) + \sum_{m=1}^{\infty} f_m(\eta), \quad (46)$$

$$\hat{g}(\eta) = g_0(\eta) + \sum_{m=1}^{\infty} g_m(\eta), \quad (47)$$

$$\hat{\theta}(\eta) = \theta_0(\eta) + \sum_{m=1}^{\infty} \theta_m(\eta), \quad (48)$$

$$\hat{\phi}(\eta) = \phi_0(\eta) + \sum_{m=1}^{\infty} \phi_m(\eta). \quad (49)$$

Eqs. (46)-(49) have the general solutions in the forms

$$f_m(\eta) = f_m^*(\eta) + C_1 + C_2 \exp(\eta) + C_3 \exp(-\eta), \quad (50)$$

$$g_m(\eta) = g_m^*(\eta) + C_4 + C_5 \exp(\eta) + C_6 \exp(-\eta), \quad (51)$$

$$\theta_m(\eta) = \theta_m^*(\eta) + C_7 \exp(\eta) + C_8 \exp(-\eta), \quad (52)$$

$$\phi_m(\eta) = \phi_m^*(\eta) + C_9 \exp(\eta) + C_{10} \exp(-\eta), \quad (53)$$

where $f_m^*(\eta), g_m^*(\eta), \theta_m^*(\eta)$ and $\phi_m^*(\eta)$ denotes the special solutions. The auxiliary parameters $\hbar_f, \hbar_g, \hbar_\theta$ and $\hbar_\phi$ for the functions f, g, θ and ϕ can adjust and control the convergence of homotopic solutions. To obtain the appropriate convergence region, we plotted the $\hbar$ −curve at 15th order of approximations. It is found from Fig. 1 the range of admissible values are $-1.1 \leq \hbar_f \leq -0.15$, $-1.25 \leq \hbar_g \leq -0.1$, $-1.0 \leq \hbar_\theta \leq -0.2$ and $-1.15 \leq \hbar_\phi \leq -0.05$. Further it is noted that our series solutions converge in the whole region of η when $\hbar_f = \hbar_g = -0.6$ and $\hbar_\theta = \hbar_\phi = -0.9$.

Table 1 is made just to see that how many orders of approximations are required for a convergent solution. It is found that for velocities f and g a 15th order of solution is sufficient however for θ and ϕ the required convergence will be achieved at 30th order solution. Hence we need fewer deformations for the velocities as compared to temperatures for a convergent solution.

4. GRAPHICAL RESULTS AND DISCUSSION

The homotopy analysis method solutions in the form of an infinite series are obtained using symbolic software MATHEMATICA. The values of $\hbar$ are chosen in such a way that the obtained series is convergent for the chosen set of fluid parameters appearing in the problem. Our primary interest in this model is to see the effect of non-Newtonian fluid parameter; unsteadiness and influence of other various involve parameter on the velocity and temperature profiles. To depict the influence of different parameters on the velocity and temperature profiles Figs. 2-11 have been sketched. The variation of dimensionless parameter A of $f'(\eta)$ and $g'(\eta)$ for three dimensional flow situations is elucidating in Fig. 2. This Fig. shows that velocity field is an increasing function of A. It is also noted that the boundary layer also increases with an increase in A. Fig. 3 shows the effect of α on the velocity profile $f'(\eta)$ and $g'(\eta)$ for three dimensional situation. It is observed that from figure 3(a) the velocity $f'(\eta)$ decreases with increasing values of the stretching ratio α while the velocity $g'(\eta)$ increases by increasing the value of α (see Fig. 3(b)). It is examined that the behavior of α on $f'(\eta)$ and $g'(\eta)$ is similar in qualitative sense for steady flow situation as Hayat *et al.* [16]. The influence of parameter A on temperature profiles $\theta(\eta)$ and $\phi(\eta)$ for three dimensional flow situation is portrayed in Fig. 4. This Fig. indicates that temperature is a decreasing function of A for both CT and CH cases. It is also noted that the thermal boundary layer decreases with an increase in A. It has been observed that the variation of the sheet temperature has substantial effects on the thermal boundary layer. Fig. 5 describes the influence of Deborah number λ_1 on $\theta(\eta)$ and $\phi(\eta)$ for three dimensional flow situations. It is observed that for large values of λ_1 the system exhibits viscoelastic behavior while for small values the conventional viscous effects dominates and the situation is quite different for β_1 when λ_1 keeping fixed. It can be seen that as we increases Deborah number λ_1 it give rise the temperature profiles. It is fact that an increase in Deborah number λ_1 increases the relaxation time. The deviation of β_1 on $\theta(\eta)$ and $\phi(\eta)$ are seen in Fig. 6. Here we see that the temperature profiles decreases when we increase Deborah number β_1. An increase in Deborah number β_1 is due to increase in retardation time. An increase in retardation time decreases the temperature profiles. It is worth mentioning that the stress decreases with an increase in the relaxation parameter. Retardation parameter characterizes the retardation time when strain decreases at constant stress, so velocity decreases by increasing the retardation parameter. A comparison between Figs. 5 and 6 shows that Deborah numbers λ_1 and β_1 effects quite oppositely on temperature profiles. Fig. 7 elucidates the influences of the stretching ratio α on the temperature profiles. It is noted that the temperature profile decreases with increasing values of the stretching ratio α in both CT and CH cases. It is also observed that the thermal boundary layer is decreased for large values of the stretching ratio α. It is further noted that these results are similar in qualitative sense with the temperature profiles shown by Liu and Andersson [12]. The effect of power indices r and s on the temperature profiles are seen through Figs. 8 and 9. It can be seen that the indices r and s have similar effect on the temperature profiles. It is observed that both decrease the temperature and thermal boundary layer thickness. Fig. 10 shows the effects of the heat source/sink parameter β on the temperatures $\theta(\eta)$ and $\phi(\eta)$. As expected, the temperature increases with increasing heat source $\beta > 0$ and decreases in the case of heat sink $\beta < 0$. The behavior of Prandtl number Pr on the temperature is shown in Fig. 11. The temperature decreases with an increase in Prandtl number which implies that the thermal boundary layer becomes thinner with large Prandtl number. The Prandtl number depends on thermal diffusivity and it plays a vital role for higher and lower temperature. Hence greater value of Prandtl number reduces thermal diffusivity and consequently temperature decreases.

Table 2 shows the comparison with the existing limiting solutions in the literature. From this Table we examined that our series solutions have an excellent agreement with the previous limiting results. Numerical values of local Nusselt number $-\theta'(0)$ for different values of Pr, α, β, A, r and s in both viscous and Jeffery fluid cases are obtained in Table 3. We observed that the local Nusselt number (heat transfer rate at the wall) for viscous fluid case are quantitatively lesser in comparison than Jeffery fluid. It is also observed that an increase in the values of unsteadiness A may also increase the Nusselt number.

5. CONCLUDING REMARKS

Three dimensional unsteady flow and heat transfer characteristics of a Jeffery fluid due to an unsteady bidirectional stretching sheet is investigated in this paper. The key observations are listed below.

(i) Velocity fields $f'(\eta)$ and $g'(\eta)$ are the increasing function of time dependent parameter A.

(ii) Temperature profiles $\theta(\eta)$ and $\phi(\eta)$ are the decreasing functions of time dependent parameter A.

(iii) The Deborah numbers λ_1 and β_1 behave quite opposite for both the velocities and temperature profiles.

(iv) The constant surface temperature (CT) and constant heat flux (CH) in both cases decreases when α increases.

(v) Both temperature and thermal boundary layer thickness are decreased when the Prandtl number increases.

(vi) For $A = 0$, the steady flow situation can be obtained.

(vii) For $\lambda_1 = \beta_1 = 0$, the results for Newtonian fluid case can be recovered. 3-D flow of Jeffrey fluid in a channel with stretched wall, Europ. Phys. J. Plus, 127 (2012) 12128-5.

Table 1: Numerical values of $f''(0)$, $g''(0)$, $\theta'(0)$ and $\phi''(0)$ at different order of approximations when $\alpha = 0.4, \lambda_1 = 0.3$, $\beta = \beta_1 = 0.2, r = s = 1.0$, $Pr = 1.0$, $\hbar_f = \hbar_g = -0.6$ and $\hbar_\theta = \hbar_\phi = -0.9$.

Order of approximation	$-f''(0)$	$-g''(0)$	$-\theta'(0)$	$\phi''(0)$
1	1.191250	0.433300	1.235000	1.395000
5	1.217145	0.443713	1.382202	1.224081
10	1.217155	0.443747	1.414834	1.198861
15	1.217154	0.443746	1.425933	0.190801
20	1.217154	0.443746	1.430894	1.187282
25	1.217154	0.443746	1.431533	1.186834
30	1.217154	0.443746	1.431496	1.186533
35	1.217154	0.443746	1.431496	1.186533
40	1.217154	0.443746	1.431496	1.186533

Table 2: Numerical values of $f''(0)$, $g''(0)$, $f(\infty)$ and $g(\infty)$ for different value of α when $\beta_1 = \lambda_1 = A = 0$.

		$f''(0)$	$g''(0)$	$f(\infty)$	$g(\infty)$
Wang [8]	$\alpha = 0.0$	-1	0	1	0
Liu and Andersson [10]		-1	0	1	0
Present solution		-1	0	1	0
Wang [8]	$\alpha = 0.25$	-1.048813	-0.194564	0.907075	0.257986
Liu and Andersson [10]		-1.048813	-0.194565	0.907067	0.257966
Present solution		-1.048811	-0.194564	0.907046	0.257993
Wang [8]	$\alpha = 0.50$	-1.093097	-0.465205	0.842360	0.451671
Liu and Andersson [10]		-1.093096	-0.465206	0.842361	0.451663
Present solution		-1.093095	-0.465205	0.842386	0.451677
Wang [8]	$\alpha = 0.75$	-1.134485	-0.794622	0.792308	0.612049
Liu and Andersson [10]		-1.134486	-0.794619	0.792293	0.612128
Present solution		-1.134486	-0.794618	0.792302	0.612135
Wang [8]	$\alpha = 1.0$	-1.173720	-1.173720	0.751527	0.751527
Liu and Andersson [10]		-1.173721	-1.173721	0.751494	0.751494
Present solution		-1.173721	-1.173721	0.751497	0.751497

Table 3: Values of local Nusselt number $-\theta'(0)$ for different values of $Pr, \alpha, \beta, A, r, s, \lambda_1, \beta_1$.

α	Pr	A	β	r	s	$\lambda_1 = \beta_1 = 0.0$	$\lambda_1 = \beta_1 = 0.5$
0.25	1.0	0.5	0.0	0.0	0.0	1.069386	1.061258
0.50						1.108350	1.115748
0.75						1.158753	1.169394
0.50	0.5	0.5	0.0	0.0	0.0	0.739980	0.743691
	1.5					1.459927	1.470380
	2.0					1.773171	1.791630
0.5	1.0	0.0	0.0	0.0	0.0	0.716953	0.714504
		1.0				1.444192	1.463342
		1.5				1.754934	1.774946
0.5	1.0	0.5	-0.2	0.0	0.0	1.207769	1.214469
			0.2			0.997745	1.005936
			0.4			0.873239	0.882331
0.5	1.0	0.5	0.0	-2.0	0.0	0.340102	0.314223
				2.0		1.663113	1.681363
				4.0		2.108220	2.130246
0.5	1.0	0.5	0.0	0.0	-2.0	0.746805	0.754706
					2.0	1.412769	1.419411
					4.0	1.677609	1.683402

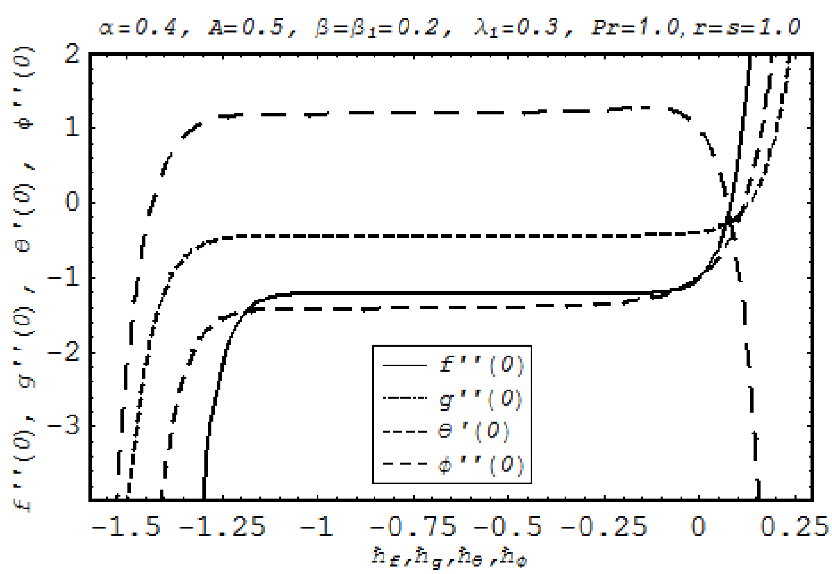

Fig. 1: The $\hbar$-curve for $f''(0), g''(0), \theta'(0)$ and $\phi''(0)$ at 15th –order of approximation.

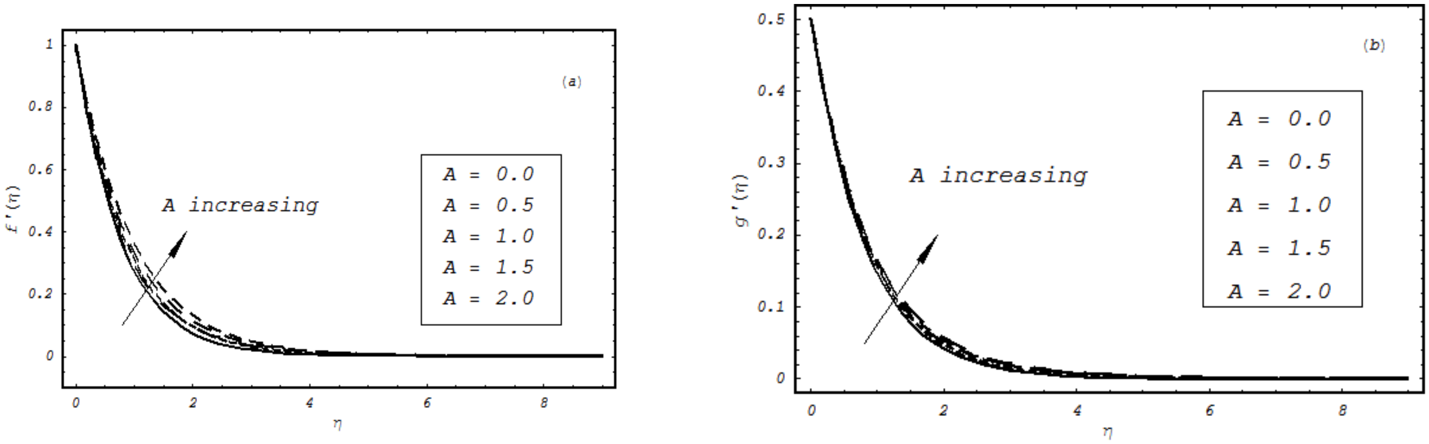

Fig. 2: **Influence of unsteadiness parameter A on velocity (a) $f'(\eta)$ case (b) $g'(\eta)$ case when $\lambda_1 = 0.3, \beta_1 = 0.2$ and $\alpha = 0.5$.**

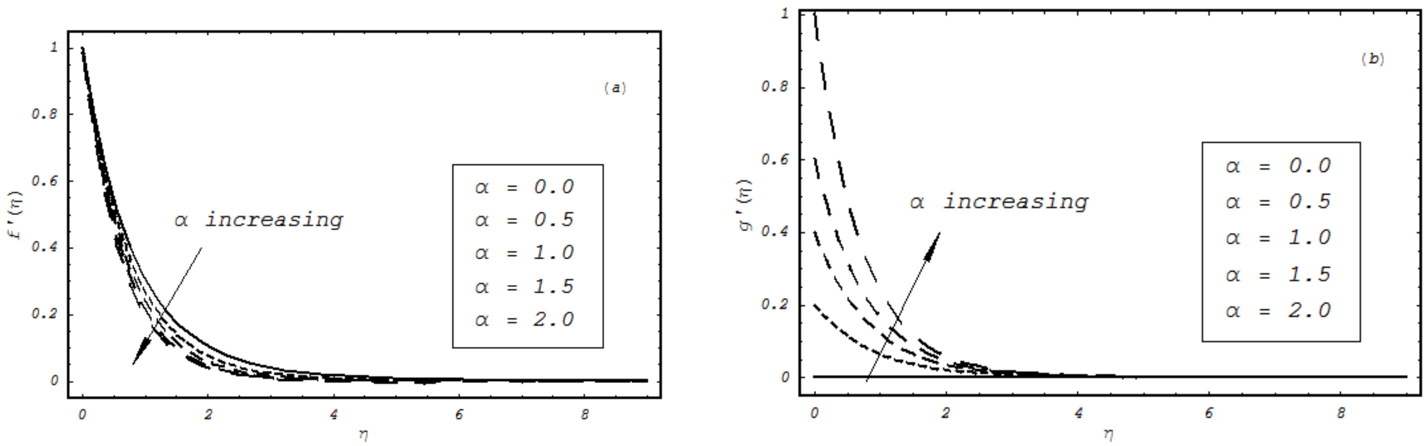

Fig. 3: **Influence of Deborah number λ_1 on temperature, (a) (a) $f'(\eta)$ case (b) $g'(\eta)$ case when $\lambda_1 = 0.3, \beta_1 = 0.2$ and $\alpha = 0.5$.**

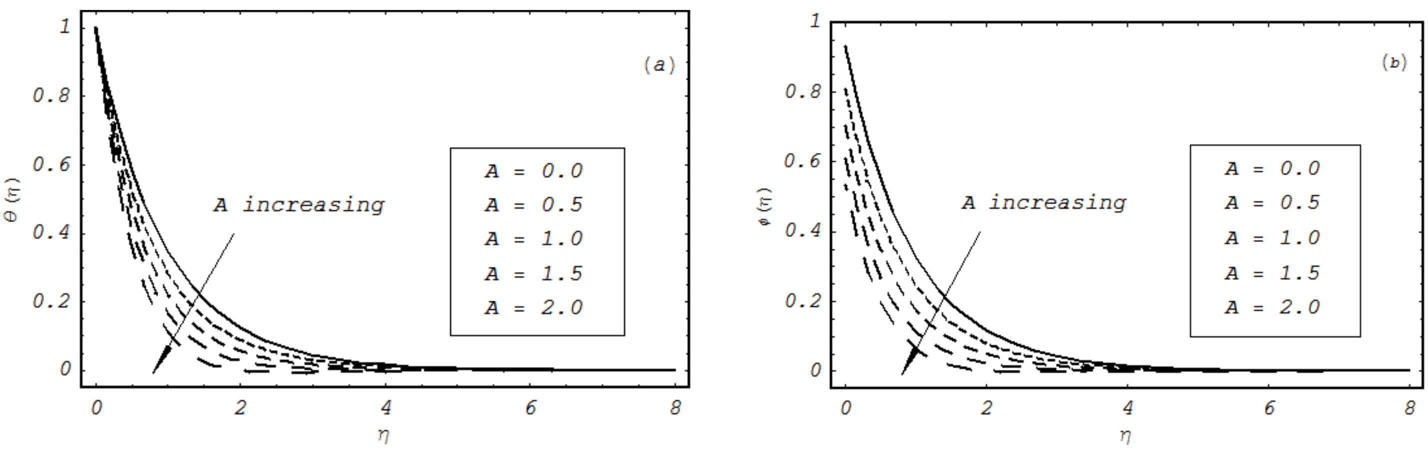

Fig. 4: **Influence of unsteadiness parameter A on temperature (a) CT case (b) CH case when $\lambda_1 = 0.3, \beta_1 = 0.2$, $Pr = r = s = 1.0$ and $\alpha = 0.5$**

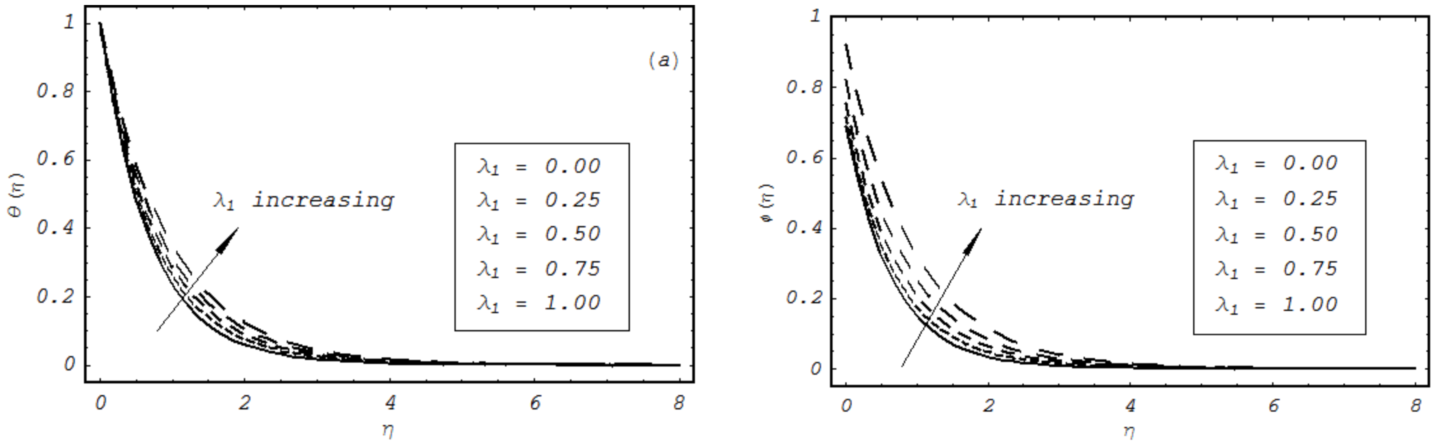

Fig. 5: Influence of Deborah number λ_1 on temperature, (a) CT case (b) CH case when $\beta_1 = 0.2$, $Pr = r = s = 1.0$ and $\alpha = 0.5$.

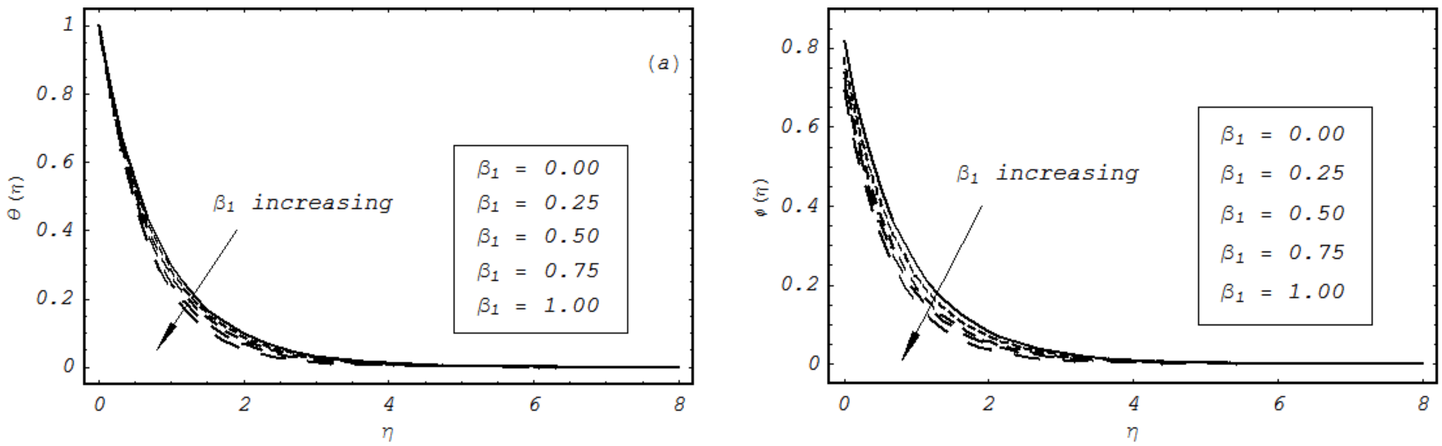

Fig. 6: Influence of Deborah number β_1 on temperature, (a) CT case (b) CH case when $\lambda_1 = 0.3$, $Pr = r = s = 1.0$ and $\alpha = 0.5$

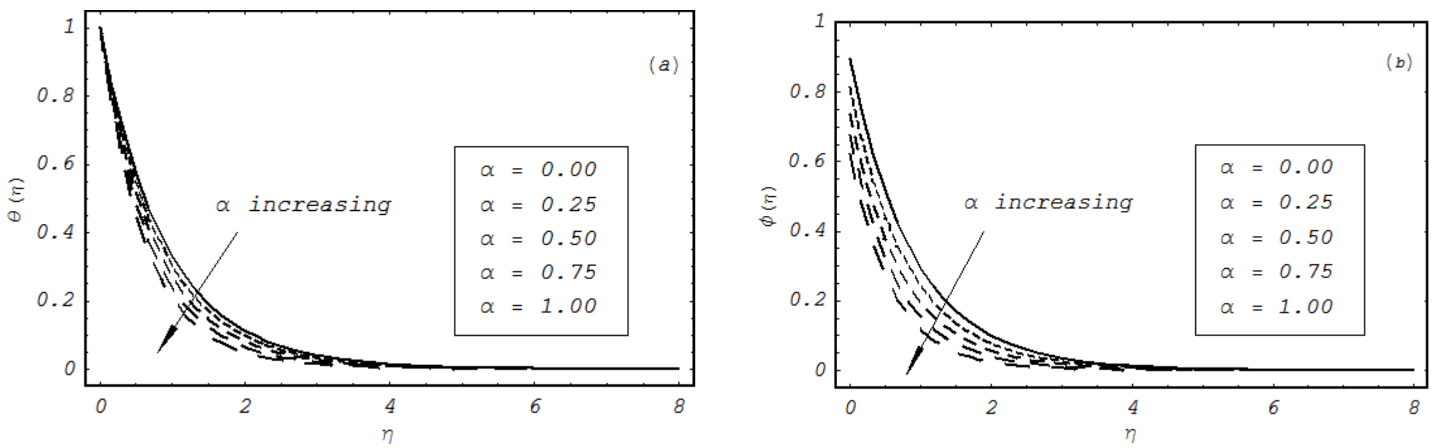

Fig. 7: Influence of stretching parameter α on temperature, (a) CT case (b) CH case when $\lambda_1 = 0.3$, $\beta_1 = 0.2$ and $\alpha = 0.5$.

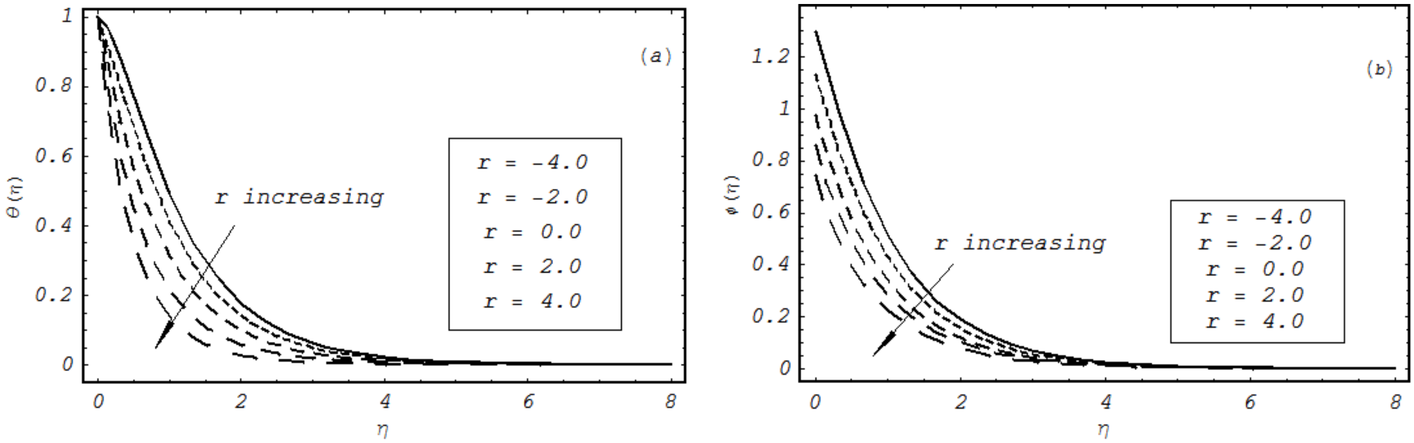

Fig. 8: Influence of r on temperature, (a) CT case (b) CH case when $\lambda_1 = 0.3$, $\beta_1 = 0.2$ and $\alpha = 0.5$.

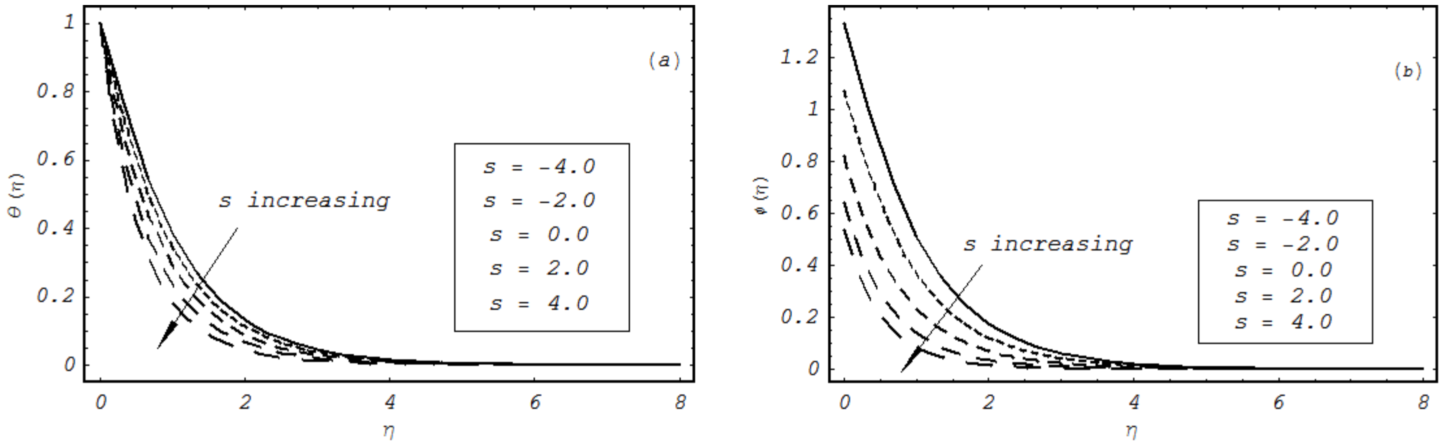

Fig. 9: Influence of s on temperature, (a) CT case (b) CH case when $\lambda_1 = 0.3$, $\beta_1 = 0.2$ and $\alpha = 0.5$.

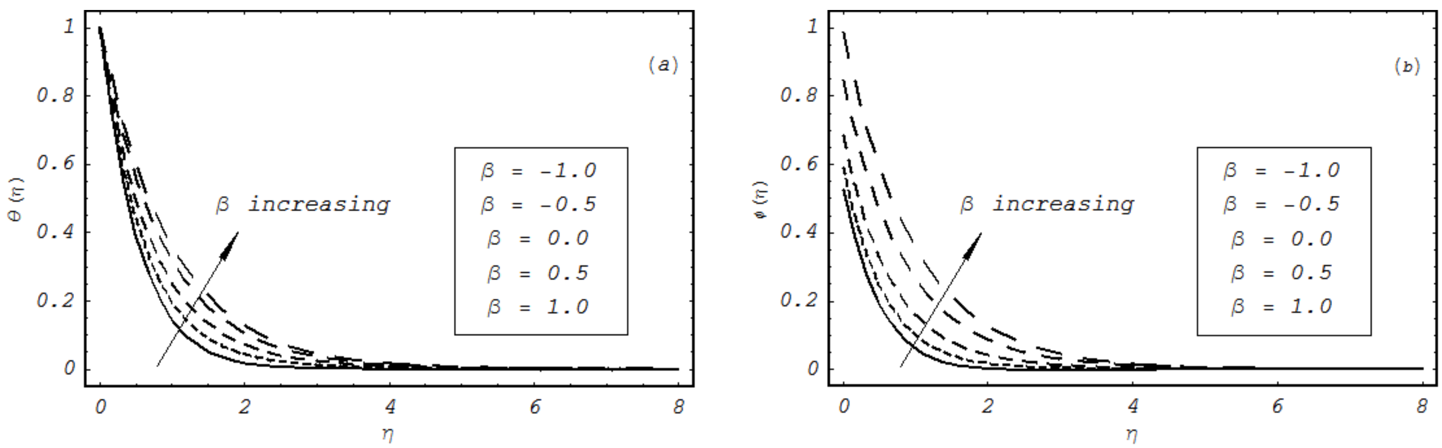

Fig. 10: Influence of β on temperature, (a) CT case (b) CH case when $\lambda_1 = 0.3$, $\beta_1 = 0.2$ and $\alpha = 0.5$.

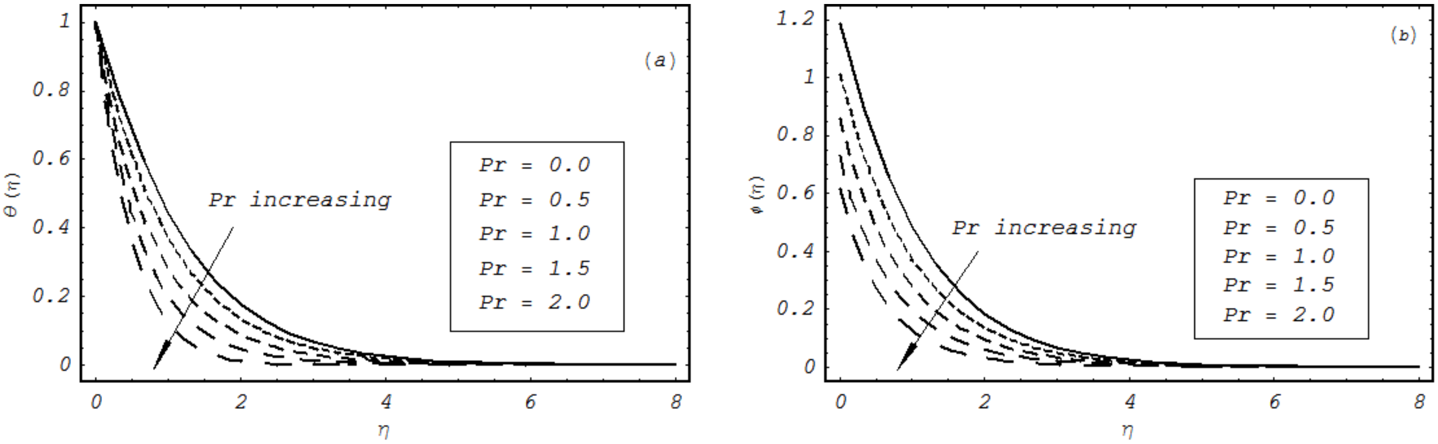

Fig. 11: Influence of Pr on temperature, (a) CT case (b) CH case when $\lambda_1 = 0.3$, $\beta_1 = 0.2$ and $\alpha = 0.5$.

REFERENCES:

[1] M. Jamil, N. A. Khan and A. Rauf, Oscillating flows of fractionalized second grade fluid, Maths ematical Physics, 2012 (2011) 1-23.

[2] M. Sajid, Z. Abbas, T. Javed and N. Ali, Boundary layer flow of an Oldroyd-B fluid in the region of stagnation point over a stretching sheet, Can. J. Phys., 88 (2010) 635-640.

[3] T. Hayat and A. Alsaedi, On thermal radiation and Joule heating effects on MHD flow of an Oldroyd-B fluid with thermophoresis, Arb. J. Sci. Eng., 36 (2011)1113-1124.

[4] T. Hayat, Z. Abbas, T. Javed and M. Sajid, "Three-dimensional rotating flow induced by a shrinking sheet for suction,"Chaos, Solitons and Fractals, 39 (2009) 1615-1626.

[5] T. Hayat, S. A. Shezad, M. Qasim and S. Obaidat, Radiative flow of Jeffery fluid in a porous medium with power law heat flux and heat source, Nuclear Engineering and Design, 243 (2012) 15-19.

[6] S. A. Shehzad, A. Alsaedi and T. Hayat, Hydromagnetic steady flow of Maxwell fluid over a bidirectional stretching surface with prescribed surface temperature and prescribed heat flux, PLoS ONE, 8(7):e68139. Doi: 10.1371.

[7] L. J. Crane, Flow past a stretching plate, Z. Angew Math. Phys., 21(4) (1970) 645-647.

[8] C. Y. Wang, The three dimensional flow due to stretching surface, Phys. Fluids, 27(1989) 1915-1917.

[9] P. D. Ariel, Generalized three dimensional flow due to stretching surface, Z. Angew. Math. Mech,. 83 (2003) 844-852.

[10] I. C. Liu, I. Andersson, Heat transfer over a bidirectional stretching sheet with variable thermal conditions, Int. J. Heat Mass Transfer, 51 (2008) 4018-4024.

[11] I. Ahmad, M. Ahmed, Z. Abbas and M. Sajid, Hydromagnetic flow and heat transfer over a bidirectional stretching surface in a porous medium, Thermal Sciences, 15 (2011) 205-220.

[12] T. Hayat, M. Sajid and I. Pop, Three-dimensional flow over a stretching surface in a viscoelastic fluid, Nonlinear Analysis: Real World Applications, 9 (2008) 1811-1822.

[13] T. Hayat, S. A. Shahzad and A. Alsaedi, Three dimensional stretched flow of Jeffery fluid with variable thermal conductivity and thermal radiation, Appl. Math. Mech., 34 (2013) 823-832.

[14] S. A. Shehzad, T. Hayat, M. S. Alhuthali and S. Asghar, MHD three dimensional flow of Jeffery fluid with Newtonian heating, J. Cent. South Uni., 21 (2014) 1428-1433.

[15] C. D. Surma Devi, H. S. Takhar, and G. Nath, Unsteady three dimensional boundary layer flow due to a stretching surface, International Journal of Heat and Mass Transfer, 29 (1986) 1996-1999.

[16] K. N. Lakshimsha, S. Venkateswaran and G. Nath, Three dimensional unsteady flow with heat and mass transfer over a continuous stretching surface, Journal of heat transfer, 110 (1988) 590-595.

[17] F. M. Ali, R. Nazar, N. M. Arifin and I. Pop, Unsteady flow across a stretching surface, International Communications in Heat and Mass Transfer, 37 (2010) 476-479.

[18] M. Abd El-Aziz, Radiation effect on the flow and heat transfer over an unsteady stretching sheet, International Communications in Heat and Mass Transfer, 36 (2009) 521-524.

[19] T. Hayat, M. Qasim and Z. Abbas, Homotopy solution for unsteady three-dimensional MHD flow and mass transfer in a porous space, Comm. Nonlinear. Sci. Num. Simul., 15 (2010) 2375–2387.

[20] T. Hayat, M. Mustafa and A. A. Hendi, Time dependent three dimensional flow and mass transfer of elastico-viscous fluid over unsteady stretching sheet, App. Math. Mech., 32 (2011) 167-178.

[21] M. Awais, T. Hayat, A. Alsaedi and S. Asghar, Time-dependent three-dimensional boundary layer flow of a Maxwell fluid, Computers & Fluids, 91 (2014) 21–27.

[22] I. Ahmad, M. Ahmad and M. Sajid, Heat transfer analysis of MHD flow due to unsteady bidirectional

stretching sheet through porous space, Thermal Sciences, doi: 10.2298/TSCI140313114A.

[23] S. J. Liao, The proposed homotopy analysis method for the solution of nonlinear problems, PhD Thesis, Shangai Jiao Tong University, (1992).

[24] S. J. Liao, Beyond perturbation: Introduction to Homotopy Analysis Method, Chapman & Hall, CRC Press, Boca Raton, (2003).

[25] T. Hayat, Z. Abbas and T. Javed, Mixed convection flow of a micropolar fluid over a nonlinear stretching sheet, Phy. Lett. A, 372 (2008) 637-647.

[26] Z. Abbas, M. Sajid and T. Hayat, MHD boundary layer flow of an upper-convected Maxwell fluid in a porous channel, Theor. Comput. Fluid Dyn., 20 (2006) 229-238.

[27] S. Abbasbandy, The application of homotopy analysis method to nonlinear equations arising in heat transfer, Phys. Lett. A, 360 (2006) 109-113.

[28] M. Sajid, T. Hayat and S. Asghar, On the analytic solution of the steady flow of a fourth grade fluid, Phys. Lett. A, 355 (2006) 18-24.[29] I. Ahmad, On unsteady boundary layer flow of a second grade fluid over a stretching sheet, Adv. Theor. Appl. Mechanics. 6 (2013) 95-105.

[30] I. Hashim, O. Abdulaziz and S. Momani, Homotopy analysis method for fractional IVPs, Comm. Nonlinear Sci. Num. Simul., 14 (2009) 674-684.

[31] T. Hayat, M. Awais, A. Alsaedi and M. S. Alhothauli, 3-D flow of Jeffrey fluid in a channel with stretched wall, Europ. Phys. J. Plus, 127 (2012) 12128-5.